Characteristics and Performance of Electroactive Paper Actuator Made with Cellulose/Polyurethane Semi-Interpenetrating Polymer Networks

Zhijiang Cai, Jaehwan Kim

Center for EAPap Actuator, Department of Mechanical Engineering, Inha University, 253 Yonghyun-Dong, Nam-Ku, Incheon 402-751, South Korea

Received 24 November 2007; accepted 5 April 2008
DOI 10.1002/app.28572
Published online 4 June 2008 in Wiley InterScience (www.interscience.wiley.com).

ABSTRACT: This article introduces a cellulose/polyurethane (PU) semi-IPN-based electroactive paper (EAPap) actuator. The fabrication process, bending actuation test, and its characteristics are explained. For the fabrication of cellulose/PU semi-IPN EAPap actuator, cotton cellulose was dissolved into *N,N*-dimethylacetamide (DMAc) and lithium chloride (LiCl) solvent system. PU prepolymer prepared by poly[di(ethylene glycol) adipate] and hexamethylene diisocyanate (HDI) was mixed with DMAc cellulose solution by stirring. The mixed solution was spin-coated on a wafer and cured to form cellulose/PU semi-IPN films using 1,1,1-tris(hudroxymethyl)propane as the crosslinker. The characteristics of the cellulose/PU semi-IPN film were investigated by FTIR, scanning electron microscopy (SEM), X-ray diffraction pattern (XRD), and tensile test. The bending actuation performance of the actuator was evaluated in terms of free bending displacement with respect to the actuation frequencies, voltages, and humidity levels. It shows a good bending actuation at room humidity condition. The actuation principle of the actuator is also discussed. © 2008 Wiley Periodicals, Inc. J Appl Polym Sci 109: 3689–3695, 2008

Key words: electroactive paper; cellulose actuator; polyurethane; semi-interpenetrating network polymer; bending displacement

INTRODUCTION

Cellulose is a representative polysaccharide and is the most abundant organic polymer that is an almost inexhaustible source of raw material for environmental friendly and biocompatible product. Some hundreds of billions of tons of cellulose are annually photosynthesized by carbon dioxide fixation on land and in sea.[1] Synthesis of cellulose has also been an important challenging project in polymer chemistry.[2] Cellulose is mostly prepared from wood pulps and cottons and sea plants. Numerous new applications of cellulose take advantage of its biocompatibility and chirality for the immobilization of proteins and antibodies for the separation of enantiomeric molecules as well as the formation of cellulose composite with synthetic polymers and biopolymer.

As one of new applications, cellulose paper has been discovered as a smart material actuating with electric field.[3] Cellulose paper was made with cellulose fibers dissolved into a solvent and cast as a sheet. Thin gold electrodes were deposited on both sides of the cellulose paper, and when an electric field was applied across the thickness of the paper, it showed a bending deformation. This cellulose paper was termed as electroactive paper (EAPap).[4] Cellulose EAPap has merits as a smart material in terms of lightweight, dryness, biodegradability, abundance, low price, large displacement output, and low actuation voltage.

In the previous research, the actuation principle was found to be a combination of piezoelectric effect associated with ordered regions of cellulose and ion migration effect. By combining piezoelectricity of cellulose and ionic migration, this oriented EAPap material will enable inexpensive and lightweight biomimetic actuators and MEMS devices. Cellulose-based EAPap material is also promising as biosensors, because it is biodegradable, biocompatible, sustainable, capable of broad chemical modification, and has high mechanical stiffness and strength.[5,6]

However, its actuator performance is sensitive to humidity: its maximum bending performance was shown at high humidity condition.[7] To overcome this drawback, a novel cellulose-based interpenetrating network polymer (IPN) film actuator is prepared. In the present investigation, we attempt to use cellulose/polyurethane (PU) semi-IPN to make EAPap actuator. Details of the cellulose EAPap fabrication are delineated. Both surface and cross section mor-

Correspondence to: J. Kim (jaehwan@inha.ac.kr).
Contract grant sponsor: Creative Research Initiatives (EAPap Actuator) of MEST/KOSEF.

phologies are photographed by scanning electron microscopy (SEM). The performance of the EAPap actuator is evaluated in terms of free bending displacement with respect to the actuation frequency, activation voltage, and humidity level. Young's moduli of the materials are evaluated to explain the mechanical performance of the actuator. The actuation principle is also discussed.

EXPERIMENTAL

Materials

Cotton cellulose (MVE, DPw 7450) was purchased from Buckeye Technologies Co., USA. Lithium chloride (LiCl; extra pure) was purchased from Junsei Chemical, Japan. Molecular sieves (4 Å, 4–8 meshes) were from Acros Organics, New Jersey, USA. Hydrochloric acid (36.5–38%), poly[di(ethylene glycol) adipate] (PDEGA) ($M_n \sim 500$), and *N*,*N*-dimethylacetamide (DMAc) (anhydrous, 99.8%) were purchased from Sigma-Aldrich, USA. Anhydrous DMAc was carefully dried with molecular sieves for a week before use. 1,1,1-Tris(hudroxymethyl)propane (TMP) and hexamethylene diisocyanate (HDI) were purchased from Fluka, Cerman.

Preparation of cellulose solution

Cotton cellulose was cut into small pieces, soaked into water overnight, squeezed, and filtered to remove the water. The same process was performed four times with methanol and one time with acetone. The treated cotton cellulose and LiCl were heated under reduced pressure at 110°C for 2 h, and the LiCl was dissolved in DMAc. Then, the cotton cellulose was mixed with LiCl-DMAc solution (cellulose/LiCl/DMAc weight ratio is 2 : 9.8 : 90) and heated at 155°C for 4 h. The transparent cellulose solution was cooled to 40°C for 2 h and then to room temperature. It was kept in sealed plastic bottle for future use.

Preparation of cellulose/PU semi-IPN EAPap

The value of NCO/OH was predetermined theoretically to be 1. Poly[di(ethylene glycol) adipate] was vacuum dried for 5 h at 110°C before use. HDI was dropped into the PDEGA at 50°C for 2 h to obtain the PU prepolymer. The mixture of PU prepolymer (2 g) and the cellulose solution (40 g) was mechanically stirred for 3 h to obtain transparent solution. Then, 1,1,1-tris(hydroxymethyl)propane was used as the crosslinker of PU prepolymer. The clear mixture solution was spin-coated on wafer and cured at room temperature for 12 h. To ensure complete elimination of the solvent, the films were then dried at 60°C for 6 h. After that, the films were washed with running tap water for 8 h and then immersed in deionized water for 24 h. Because lithium ions were entirely removed by running water, its concentration in the film was negligible. The film was took out and laid in air for 24 h. And then, the films were immersed hydrogen chloride aqueous solution (the concentration of hydrogen chloride is 1%) for 1 h and then washed with tap water and deionized water for 12 h to delete little ionic molecules. And then, the wet films were taken out from water and laid in air for 24 h. To make an EAPap actuator, gold electrodes were deposited on both sides of the cellulose/PU semi-IPN film by using a physical vapor deposition system. The size of the EAPap sample was 10 mm × 40 mm. The thickness of the gold electrodes was so thin (0.1 μm) that the gold electrodes did not significantly affect the bending stiffness of the cellulose paper.

Characterization and actuator performance

Characteristics of DMAc regenerated cellulose and cellulose/PU semi-IPN films were analyzed by FTIR, X-ray diffraction pattern (XRD), SEM, and tensile test. FTIR spectra were obtained using a PerkinElmer System 2000 FT-IR spectrophotometer. The films were cut into very little particles and characterized by a Fourier transform infrared spectrometer (FTIR) for the evaluation of chemical structures using a KBr pellet. The obtained data were transferred to the PC for the line fitting. XRD was recorded on an X-ray diffractometer (D/MAX-2500, Rigaku), by using Cu Kα radiation at 40 kV and 30 mA. The diffraction angle ranged from 5° to 40°. SEM images of the films were taken with a microscope (Hitachi S-4200, Japan) to study the morphological difference of the films. The surface and cross section of the films were sputtered with gold and then observed and photographed. Tensile test specimens were prepared by cutting the membranes to 10 mm wide and 65-mm long strips using a precise cutter. Young's moduli of samples were found from the tensile test results conducted according to ASTM D-882-97 as a standard test method for tensile elastic properties of thin plastic sheeting. Tensile test was done on a universal testing machine. Two ends of the specimens were placed between the upper and lower jaws of the instrument, leaving a length of 50 mm of the film in between the two jaws. Extension speed of the instrument was 10 mm/min. The test was performed in room condition.

The actuator performance was conducted in an environmental chamber that can control temperature and humidity. The bending-displacement measurement system consists of a high precision laser doppler vibrometer (LDV) (Brüel and Kjær, 8336), an environmental chamber (KMS, CTH3-2S), a current

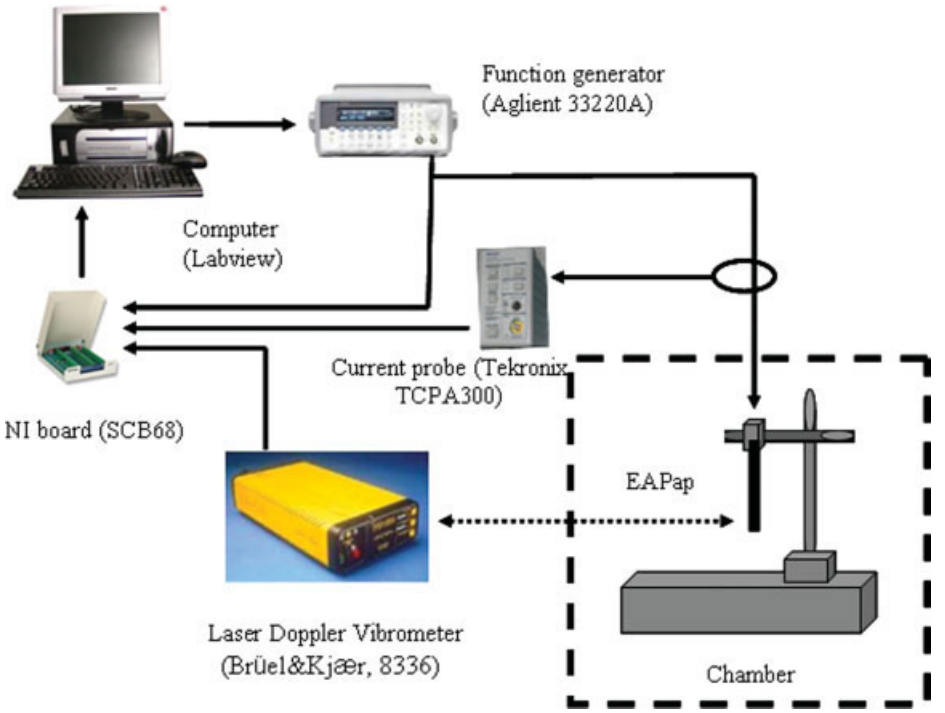

Figure 1 Computerized setup for bending displacement measurement of EAPap. [Color figure can be viewed in the online issue, which is available at www.interscience.wiley.com.]

probe (Tektronix, TCP 300), Labview software on a personal computer and a function generator (Agilent, 33220A). An EAPap actuator is supported vertically in air. Function generator controlled by computer sends out the excitation AC voltage. The input signal generated from the function generator is applied to the EAPap actuator, and it produces a bending deformation. The bending displacement of the EAPap sample is measured by the high-precision LDV mounted on an optical table, and the LDV signal is converted to the displacement through the Labview software. Simultaneously, the current probe measures the input current supplied from the function generator. The measured current signal is also analyzed simultaneously by the computer (Fig. 1).

RESULTS AND DISCUSSION

SEM observation can give information of the morphological change and miscibility. The SEM images of the surface and cross section of the DMAc regenerated cellulose and cellulose/PU semi-IPN films are shown in Figure 2. For pure DMAc-regenerated cellulose film, the surface morphology is very uniform and smooth; the cross section morphology is typical layer-by-layer structure [Fig. 2(b)]. For cellulose/PU semi-IPN film, the complicated domain structure indicates the presence of phase separation in this system. From the surface SEM image, we can see a network structure, which is attributed to the PU phase. This obvious phase separation may be due to the significant chemical structure difference between the cellulose and PU, which eventually leads to poor miscibility. From the cross section SEM images, we can see that the layer-by-layer structure becomes loose and irregular [Fig. 2(d)]. Generally, we can calculate the average width between each layer using four SEM images with large magnitude (the SEM images are not presented). For pure DMAc-regenerated cellulose film, the average width between each layer is about 50 $\pm$ 4 nm, whereas for cellulose/PU semi-IPN film, the average width between each layer increases to 200 $\pm$ 30 nm. The reason might be due to the fact that the process of cellulose regeneration and PU network formation happen simultaneously, and PU molecules and cellulose molecules can interpenetrate with each other to form a cellulose/PU semi-IPN.

The FTIR spectrum of celluloe/PU semi-IPN is shown in Figure 3. The broad band at 3450 cm^{-1} is attributed to O—H stretching vibration. Band at 2820 cm^{-1} represents the aliphatic C—H stretching vibration. Band observed at 1080 cm^{-1} is due to the presence of C—O—C stretching vibrations. *N*—H stretching vibration band is located at 3420 cm^{-1}, which is combined with O—H stretching vibration band. The peak assigned to free —NCO groups located at 2270 cm^{-1} disappear, indicating that —NCO groups located at 2270 cm^{-1} reacted with —OH groups. Meanwhile, the new absorbance peaks at wave numbers 1627 cm^{-1} and 1727 cm^{-1} are attributed to free carbonyl stretching vibration and the hydrogen-bonded carbonyl stretching vibration.

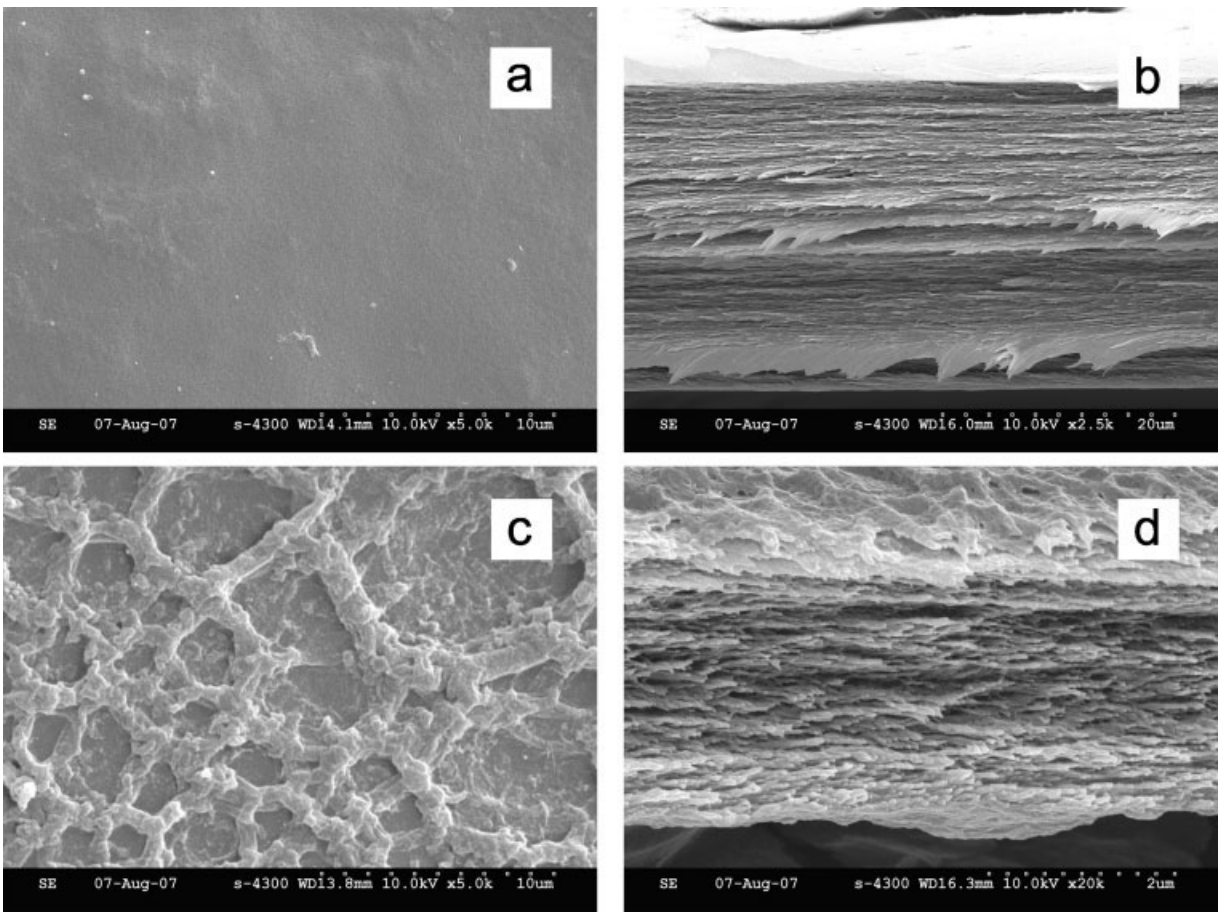

Figure 2 Scanning electron micrograph images of regenerated cellulose (a: surface; b: cross section) and cellulose/polyurethane semi-IPN (c: surface; d: cross section).

This new-formed carbonyl group indicated that the diisocyanate groups reacted with hydroxyl group to form PU network.

Figure 4 shows XRDs of DMAc-regenerated cellulose and cellulose/PU semi-IPN film. Cellulose II is well known to be a thermodynamically stable crystalline cellulose allomorph. Originally, X-ray diffraction peaks of cellulose II appear at 12.1°, 19.8°, and 22° assigned to (1 1 0), (1 $\bar{1}$ 0), and (2 0 0). From Figure 3, we can see three peaks located at 11.8°, 19.6°,

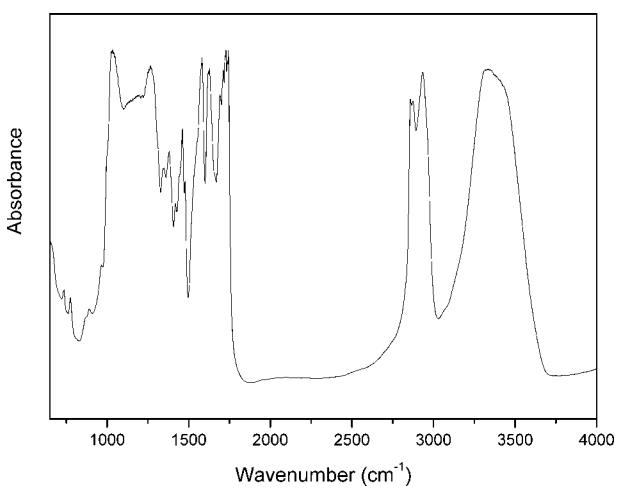

Figure 3 FTIR spectrum of cellulose/polyurethane semi-IPN.

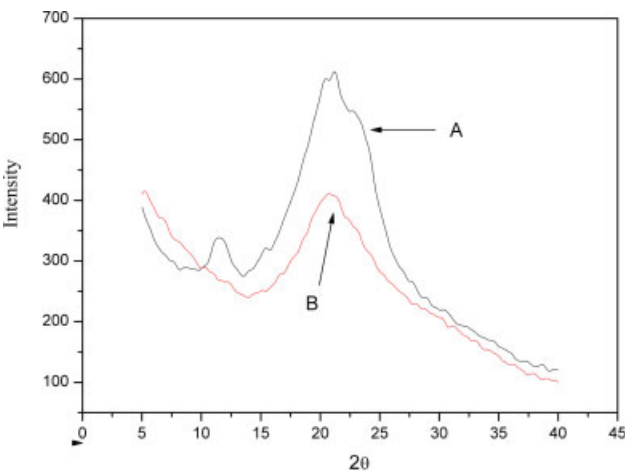

Figure 4 X-ray diffraction pattern of (A) regenerated cellulose and (B) cellulose/polyurethane semi-IPN films. [Color figure can be viewed in the online issue, which is available at www.interscience.wiley.com.]

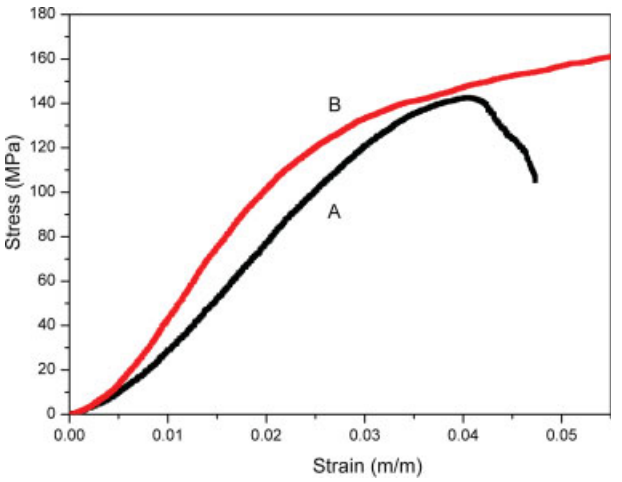

Figure 5 Stress-strain curves of (A) regenerated cellulose and (B) cellulose/polyurethane semi-IPN films. [Color figure can be viewed in the online issue, which is available at www.interscience.wiley.com.]

and 21.6° for DMAc-regenerated cellulose film, which should represent cellulose II crystalline structure. However, this crystalline diffraction peaks cannot be observed at the cellulose/PU semi-IPN film. The (1 1 0) peak at $2\theta = 11.8°$ disappeared. The (1 $\bar{1}$ 0) peak at $2\theta = 19.6°$ and the (2 0 0) peak at $2\theta = 21.6°$ were combined to form a new peak at $2\theta = 20.6°$. Compared with (1 $\bar{1}$ 0) peak and (2 0 0) peak, this new peak was changed to blunt, and the intensity was also decreased sharply. This means that some structural change may have happened for cellulose/PU semi-IPN, which may be associated with the hindrance of the crystallization of cellulose by PU network. In other words, crystallization of cellulose during regeneration is hindered by the formation of PU network due to cellulose molecules interpenetrating the PU network to form semi-IPN. In the result, this leads to a structure, which contains considerably more of the amorphous region. With the amorphous region increasing, ion mobility is increased, which could improve ion migration effect in EAPap actuator.

To investigate the mechanical characteristic of DMAc-regenerated cellulose and cellulose/PU semi-IPN films, the tensile test was performed according to ASTM D-882-97 standard test method. Figure 5 shows the stress–strain curves of the test samples. Both samples exhibit typical brittle properties. The tensile strength is about 140 and 160 MPa, and the elongation at break is about 4.5 and 5.5% for the DMAc-regenerated cellulose and cellulose/PU semi-IPN films, respectively. The Young's modulus found from the slope of the curves was 4.2 and 5.7 GPa for the DMAc-regenerated cellulose and cellulose/PU semi-IPN films. Compared with DMAc-regenerated cellulose, the Young's modulus, tensile strength, and the elongation at break were increased for cellulose/PU semi-IPN film. This is may be due to the formation of the IPN; nevertheless, this does not change the brittle characteristic of the DMAc-regenerated cellulose. Young's modulus values can be used to calculate the stiffness and resonance frequency of the samples.

The movement direction of cellulose/PU semi-IPN-based EAPap actuator in the presence of DC voltage is shown in Figure 6. Upon the DC voltage (4 V), the tip of the EAPap sample moved from the

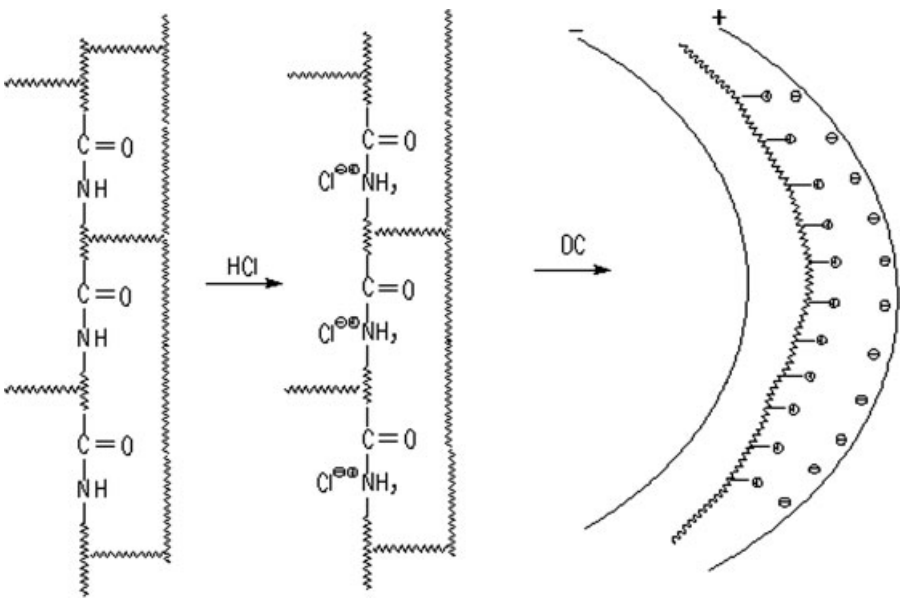

Figure 6 Actutuion behavior of cellulose/polyurethane semi-IPN based actuator under DC voltage: (a) polyurethane network chains, (b) when hydrogen chloride acid was added, and (c) when a DC electric field was applied.

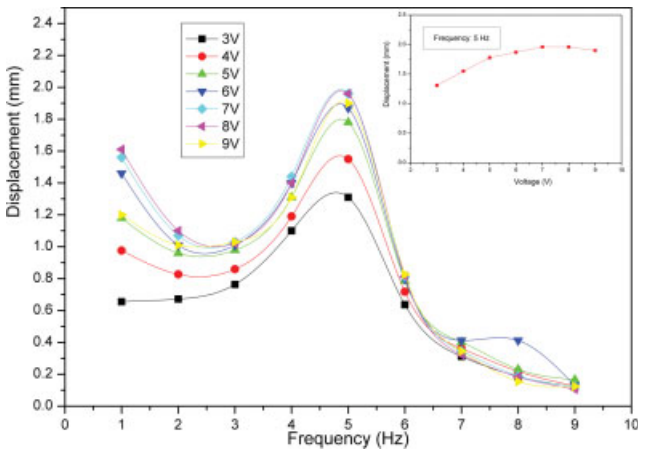

Figure 7 Bending displacements with variation of activation voltage and frequency at room condition. [Color figure can be viewed in the online issue, which is available at www.interscience.wiley.com.]

vertical position to the negative electrode (cathode). The moving speed was rather slow. When the power is turned off, the tip of the EAPap sample stopped and returned to the original place after a long period of time. The actuation principle can be explained from Figure 6. The cations ($—N^+H_2—$) connected with polymer molecular chain could not move freely, but the anions (Cl^-) are free to move approximately. On the low-DC voltage condition, the cations cannot nearly move to negative electrode, whereas the anions can move to positive electrode. As the anions move and assemble at anode, the repelling force between the anions (Cl^-) makes the film bend to negative electrode.

The bending displacement of cellulose/PU semi-IPN-based actuator was measured at the tip of the samples with the laser vibrometer. The test was performed as a function of frequency under different activation voltage at room condition and relative humidity (RH) as 70, 80, and 90%, respectively. Figure 7 represents the displacement outputs of the actuator measured with respect to the excitation frequency at different excitation voltage (peak to peak) at room condition (25°C ± 0.5°C and 30% ± 2% RH). The variation of bending displacement at the resonance frequency of 5 Hz with the activation voltage is represented in zoomed-in figure. When the excitation voltage is below 7 Vpp, the tip displacement tends to increase linearly along with the excitation voltage. After that, with the excitation voltage increasing, the tip displacement changes little, and the maximum bending displacement of 1.96 mm is achieved at 7 Vpp and 5 Hz.

Figure 8 shows the humidity effect on the bending displacement output for cellulose/PU semi-IPN-based actuator. Sample was humidified to three RH levels (70, 80, and 90% RH), and the displacement is shown as a function of excitation voltage, frequency, and humidity. All tests were performed under the control of temperature at 25°C. Figure 8(a) shows the measured bending displacement with different RH levels and actuation voltage at the fixed frequency of 4 Hz. The tendency is same to room condition. The displacement tends to increase linearly with the actuation voltage increasing. Figure 8(b) shows the measured bending displacement with different RH levels and actuation frequency at the fixed voltage of 6 V. The displacement is increased when the humidity level increased, and the maximum output is reached at 90% RH. The reason might be due to the increase of ionic mobility in the actuator. When the humidity increases, the water content in the actuator increases, and it results in softening the actuator and making the anions easier to move. On the

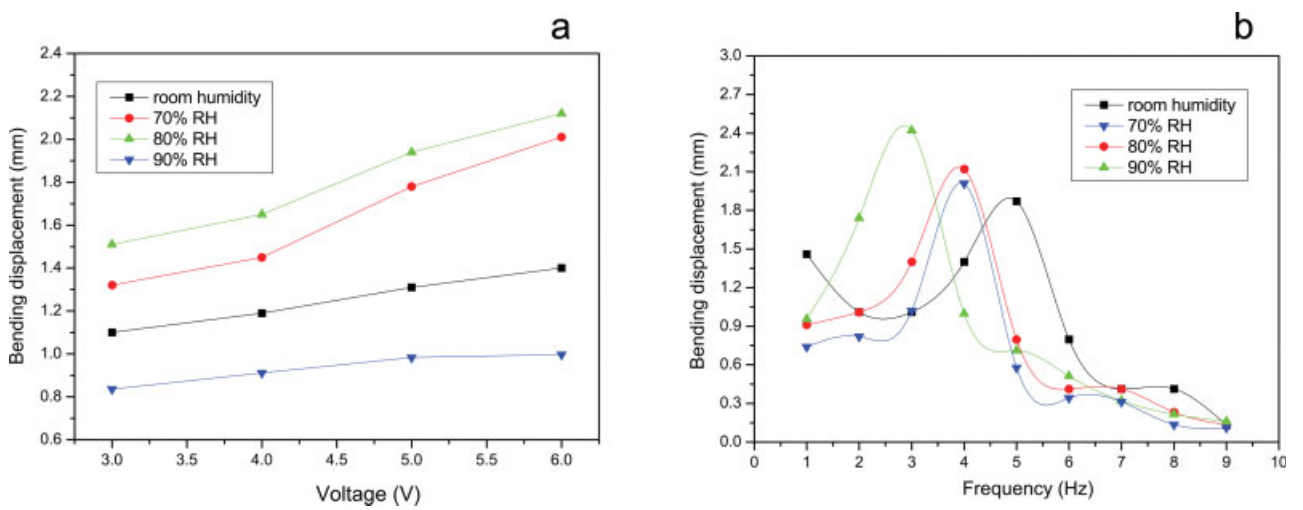

Figure 8 Humidity effect on the bending displacements: a variation of actuation voltage (25°C, 4 Hz); b variation of frequency (25°C, 6 V). [Color figure can be viewed in the online issue, which is available at www.interscience.wiley.com.]

other hand, the resonance frequency is decreased as the humidity level is increased. As seen form Figure 8(b), the resonance frequency is shifted from 5 Hz for room condition to 3 Hz for 90% RH. Resonance frequency of EAPap actuator can be theoretically calculated based on the classical beam theory.[8] Supposing the gold electrode layer is so thin ($\sim$ 100 nm) that its stiffness is negligible, the resonance frequency of the EAPap actuator is proportional to the root of Young's modulus.[9] Usually, the Young's modulus of the film decreases when the humidity in the film is increased. According to literature,[10] the Young's modulus is reduced to nearly half when the RH is 99% RH. In this case, the main reason for resonance frequency decreased is the Young's modulus decreased with humidity level increased. In summary, when the humidity level is increased, the ion mobility increases and the stiffness decreases, which results in a large bending displacement.

The working principle of actuators is mainly divided into two parts. In our previous work, based on the cellulose structure and the fabrication technology, the actuation principle of cellulose EAPap has been claimed to be a combination of ion migration effect and piezoelectricity effect, which is associated with selective ionic and water transport and dipole moment of the constitutes of cellulose EAPap.[4]

For cellulose/PU semi-IPN-based actuator, the ion migration effect as well as the piezoelectric effect could be claimed also as the actuation principle. As seen from XRD results, the ordered domains of cellulose in cellulose/PU semi-IPN decreased, which may cause a decrease in piezoelectric effect. At the same time, with the amorphous region increasing the cellulose can absorb more water to improve the ions mobility. Furthermore, the cellulose layer-by-layer structure becomes irregular and loose, which is in favor of ion migration. The introduction of PU network can also improve ion migration effect, because the PU molecules can make cations ($—N^+H_2—$) fixed on molecular chain while anions (Cl^-) can move freely. All these factors make the ion migration effect playing a more important role than piezoelectric effect in cellulose/PU semi-IPN-based actuator.

CONCLUSIONS

A cellulose/PU semi-interpenetrating polymer networks based EAPap actuator was fabricated, and its actuator performance and characteristics were tested. Cotton cellulose was dissolved in DMAc/LiCl solvent system, and PU prepolymer was dispersed uniformly by using strong mechanical stir. SEM images and XRDs indicated that PU network is formed, and the crystallinity of cellulose decreases at the same time. Tensile test results showed that Young's modulus increased by 34% with the formation of semi-IPN in the cellulose.

The actuator performance test of cellulose/PU semi-IPN-based EAPap actuator was carried out with frequency, voltage, and humidity variations. The bending displacement output was increased as the voltage and humidity increased. In room condition, the maximum bending displacement is about 1.96 mm achieved at 7 Vpp and 5 Hz. This value is much higher than that of the cellulose EAPap[3] in same condition. However, in high humidity level (such as 90% RH) the maximum bending displacement is lower than that of the cellulose EAPap.[3] This might indicate that this cellulose/PU semi-IPN-based EAPap actuator is more suitable to be used in low humidity level. Based on these results, the ion migration effect might play a more important role in actuation principle.

References

1. Klemm, D.; Heublein, B.; Fink, H.-P.; Bohn, A. Angew Chem Int Ed 2005, 44, 3358.
2. Kobayashi, S. J Polym Sci Part A: Polym Chem 2005, 43, 693.
3. Kim, J.; Yun, S.; Ounaies, Z. Macromolecules 2006, 39, 4202.
4. Kim, J.; Seo, Y. B. Smart Mater Struct 2002, 11, 355.
5. Deshpande, S. D.; Kim, J.; Yun, S. Smart Mater Struct 2005, 14, 876.
6. Deshpande, S. D.; Kim, J.; Yun, S. Synth Met 2005, 14, 53.
7. Kim, J.; Song, C. S.; Yun, S. Smart Mater Struct 2006, 15, 719.
8. Rao, S. S. Mechanical Vibrations, 2nd ed.; Addison-Welsy: Reading, MA, 1990; p 398.
9. Tahhan, M.; Truong, V. T.; Spinks, G. M.; Wallace, G. G. Smart Mater Struct 2003, 12, 626.
10. Mark, R. E. Handbook of Physics and Mechanical Testing of Paper and Paperboard; Dekker: New York, 1989.